International Journal of Theoretical and Mathematical Physics 2025, 15(2): 43-56
DOI: 10.5923/j.ijtmp.20251502.03

Analysis of Natural Convection along a Vertical Flat Plate with Temperature-Dependent Viscosity and Thermal Conductivity under Heat Conduction and Viscous Dissipation

Md. Al- Amin, Md. Mahmud Alam, Sree Pradip Kumer Sarker*

Department of Mathematics, Dhaka University of Engineering and Technology, Gazipur, Bangladesh

Abstract This study presents a comprehensive analysis of natural convection flow along a vertical flat plate, incorporating the effects of temperature-dependent viscosity and thermal conductivity, with additional consideration of internal heat conduction and viscous dissipation. The governing equations of continuity, momentum, and energy are formulated to include variable thermophysical properties and are solved numerically under appropriate boundary conditions using an implicit Crank–Nicolson finite difference scheme. The influence of variable viscosity and thermal conductivity on the development of thermal boundary layers, velocity profiles, temperature distributions, and local Nusselt number is systematically investigated. Results reveal that neglecting the temperature dependence of viscosity and thermal conductivity may lead to significant inaccuracies in predicting flow behavior and heat transfer performance. The analysis highlights that enhanced thermal conductivity intensifies heat transfer, while increased viscosity variation notably alters velocity gradients near the wall. This investigation contributes to the development of more accurate predictive models for natural convection-driven thermal systems and offers practical insights relevant to thermal management applications such as electronics cooling, energy systems, and passive ventilation technologies. This numerical study can be explored for different mathematical model. This study can be expanded considering Magneto hydrodynamics, for unsteady flows, considering different physics like radiation effects. This analysis can be extended by considering the moving surface.

Keywords Natural Convection, Dependent viscosity, Thermal Conductivity, Heat Conduction, Viscous Dissipation, Joule Heating

1. Introduction

Investigating the interplay between key thermophysical properties and convective heat transfer has long been a subject of both academic interest and practical importance in the fields of fluid dynamics and heat transfer. Among these properties, viscosity and thermal conductivity significantly influence fluid behavior and thermal transport characteristics. In recent years, increasing attention has been directed toward understanding how temperature-dependent variations in viscosity and thermal conductivity affect natural convection, particularly in scenarios involving vertical flat plates subjected to Joule heating and internal heat conduction. This study aims to advance that understanding by analyzing the complex coupling between these variable properties and convective phenomena using robust numerical techniques.

* Corresponding author:
pradip.duet@gmail.com (Sree Pradip Kumer Sarker)
Received: Aug. 7, 2025; Accepted: Sep. 2, 2025; Published: Oct. 31, 2025
Published online at http://journal.sapub.org/ijtmp

By incorporating temperature-dependent viscosity and thermal conductivity into the governing equations, and solving them under realistic boundary conditions, this work seeks to reveal the nuanced effects these parameters have on velocity fields, thermal boundary layers, and heat transfer efficiency. Such insights are critical for optimizing the thermal performance of engineering systems where natural convection plays a dominant role, including passive cooling technologies, electronic thermal management, and energy-efficient building design. The subsequent sections of this paper detail the mathematical formulation, numerical solution methodology, and key findings of the investigation. Through this analysis, the study contributes to the broader effort to develop more predictive and application-oriented models for natural convection processes in the presence of variable thermophysical properties. Sarker et al. [1] investigated the Variable viscosity and thermal conductivity's effects on magneto hydrodynamic (MHD) natural convection flow in a vertical flat plate. Alam et al. [2] examined the impact of a vertical flat plate with heat

conduction, pressure stress work, and viscous dissipation in natural convection flow. Alim et al. [3] examined the effect of Joule heating on the coupling of conduction with magneto hydrodynamic (MHD) free convection flow from a vertical flat plate. Rahman et al. [4] demonstrated the effects of temperature-dependent thermal conductivity on magneto hydrodynamic (MHD) free convection flow and a vertical flat plate with heat conduction.

Alim et al. [5] investigated the combined effects of viscous dissipation and Joule heating on the coupling of conduction and free convection. Molla et al. [6] examined the natural convection laminar flow with temperature-dependent viscosity and thermal conductivity and a vertically wavy surface. Safiqul Islam et al. [7] demonstrated the effects of temperature -dependent thermal conductivity on natural convection flow along a vertical flat plate with heat generation. Kabir et al. [8] examined the effects of viscous dissipation on magneto hydrodynamic (MHD) spontaneous convection flow along a vertical wavy surface. Hossain [9] examines the effects of viscous and Joule heating on magneto hydrodynamic (MHD) free convection flow with varying plate temperature. Soundalgekar et al. [10] investigate the transient free convection on an isothermal flat plate using finite difference analysis. Elbashbeshy et al. [11] analyse a steady free convection flow down a vertical plate with changing viscosity and thermal diffusivity. Kafoussius et al. [12] explore the numerical investigation of the mixed free and forced convective laminar boundary layer flow past a vertical isothermal flat plate with temperature dependent viscosity.

Anwar Hossain et al. [13] present the influence of radiation on the free convection flow of fluid with changing viscosity from a porous vertical plate. In the situation of unsteady flow, Seddeek [14] investigates the impact of varying viscosity on a magneto hydrodynamic (MHD) free convection flow past a semi-infinite flat plate with an aligned magnetic field. G. Palani Kwan et al. [15] calculated A numerical investigation on a vertical plate with changing viscosity and heat conductivity. Siattery JC [16] investigated Momentum, energy and mass transfer in continua. Ockendon H, Ockendon JR. [17] investigated Variable viscosity flows in heated and cooled channels. Elbashbeshy EMA, Dimian MF [18] computed the effects of radiation on the flow and heat transfer over a wedge with variable viscosity. Seddeek MA, Abdelmeguid MS. [19] investigated the effects of radiation and thermal diffusivity on heat transfer over a stretching surface with variable heat flux Balamurugan, K. and Karthikeyan, R [20] studied viscous dissipation effect on steady free convection flow past a semi-infinite flat plate in the presence of magnetic field. Borah, G. and Hazarika, G. C. [21] calculated the effects of variable viscosity & thermal conductivity on steady free convection flow along a semi-infinite vertical plate (in presence of uniform transverse magnetic field). Abdel-Rahman, G. M. [22] investigated the effects of variable viscosity and thermal conductivity on unsteady MHD flow of non-Newtonian fluid over a stretching porous sheet.

Alam, M. M., Alim, M. A. and Chowdhury, M. M. K. [23] investigated free convection from a vertical permeable circular cone with pressure work and non-uniform surface temperature. Aktar, S., Mahmuda Binte Mostafa Ruma and Alim, M. A. [24] calculated the conjugate effects of heat and mass transfer on natural convection flow along an isothermal sphere with radiation heat loss was. Nasrin, R. and Alim, M. A. [25] studied the MHD free convection flow along a vertical flat plate with thermal conductivity and viscosity depending on temperature. Miraj et al. [26] calculated the effects of viscous dissipation and radiation on natural convection flow on a sphere in presence of heat generation. Haque et al. [27] investigated the effects of viscous dissipation on Natural convection flow over a sphere with temperature dependent thermal conductivity. Gebhart, B. [28] studied the effects of viscous dissipation in natural convection. Based on experimental analysis, an analytical solution for the dependent thermal conductivity and variable viscosity in natural convection flow over a vertical flat plate in the presence of heat conduction will be created in this work. A. Pozzi, and M. Lupo, [29] investigated the coupling of conduction with laminar natural convection along a flat plate. Al-Mahasne Mayas Mohammad et al. [30] calculated the variable Temperature Plate Heat Transfer: MHD Fluid Natural Convection Flow in Porous Medium. Journal of Advanced Research in Numerical Heat Transfer. Iqbal Athal et al. [31] studied the Viscosity dissipation and mixed convection flow in a vertical double-passage channel with permeable fluid. Md. Farhad Hasan et al. [32] calculated the Natural Convection Flow over a Vertical Permeable Circular Cone with Uniform Surface Heat Flux in Temperature-Dependent Viscosity with Three-Fold Solutions within the Boundary Layer. Sujit Mishra et al. [33] studied Thermal performance of nanofluid flow along an isothermal vertical plate with velocity, thermal, and concentration slip boundary conditions employing buongiorno's revised non-homogeneous model. East European Journal of Physics. Uzma Ahmad et al. [34] investigated the Effects of temperature dependent viscosity and thermal conductivity on natural convection flow along a curved surface in the presence of exothermic catalytic chemical reaction.

The governing momentum and energy equations are discretized using central difference approximations for both spatial coordinates in their non-dimensional form. To solve these equations, an implicit finite difference scheme based on the Crank–Nicolson method—recognized for its numerical stability and convergence—has been employed. A custom computational code was developed to simulate the flow and thermal behavior of the system under varying conditions. The analysis yields detailed results for velocity and temperature distributions, local and average skin friction coefficients, and local and average Nusselt numbers across a range of parameters, including temperature-dependent viscosity and thermal conductivity, heat generation, viscous dissipation, Joule heating, and the Prandtl number.

By integrating the effects of internal heat conduction and Joule heating into the numerical model, this study offers a comprehensive understanding of the fundamental mechanisms governing complex convective heat transfer

processes. The insights derived are particularly relevant for improving predictive modeling in thermal-fluid systems, with practical applications in environmental control, electronic cooling, and renewable energy technologies. Understanding the influence of temperature-dependent fluid properties on natural convection along vertical surfaces is essential for optimizing thermal performance, enhancing energy efficiency, and mitigating thermal management challenges in advanced engineering systems.

2. Mathematical Analysis

This study addresses the unsteady, laminar flow of a viscous, incompressible fluid along a semi-infinite vertical flat plate. The coordinate system is defined such that the *x*-axis is aligned vertically upward along the plate surface, while the *y*-axis extends perpendicularly from the leading edge of the plate, as illustrated in Figure 1. The origin is located at the leading edge of the plate. All thermophysical properties of the fluid are considered constant, except for the density in the buoyancy term of the momentum equation, where the Boussinesq approximation is applied. Additionally, the thermal conductivity is assumed to vary linearly with temperature, while the fluid viscosity exhibits an exponential dependence on temperature. The problem also can be solved improved analytical analysis via perturbation methods for small variations in viscosity and thermal conductivity.

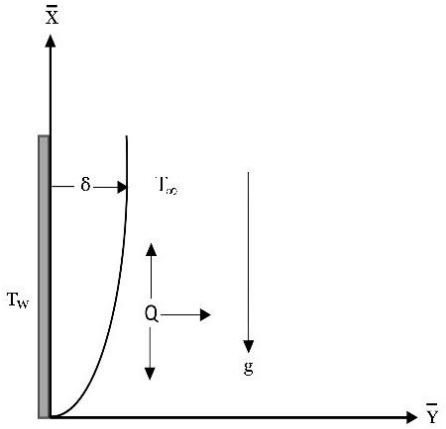

Figure 1. Geometry

The mathematical statement of the basic conservation laws of mass, momentum and energy for the steady viscous incompressible and electrically conducting flow, after simplifying we have the equation of continuity

$$\frac{\partial \bar{u}}{\partial \bar{x}}+\frac{\partial \bar{v}}{\partial \bar{y}}=0 \tag{1}$$

The equation of momentum

$$\frac{\partial \bar{u}}{\partial t'}+\bar{u}\frac{\partial \bar{u}}{\partial \bar{x}}+\bar{v}\frac{\partial \bar{u}}{\partial \bar{y}}=\frac{1}{\rho}\frac{\partial}{\partial \bar{y}}\left(\mu\frac{\partial \bar{u}}{\partial \bar{y}}\right)+g\beta\left(T'-T'_{\infty}\right) \tag{2}$$

And the equation of energy

$$\frac{\partial T'}{\partial t'}+\bar{u}\frac{\partial T'}{\partial \bar{x}}+\bar{v}\frac{\partial T'}{\partial \bar{y}}=\frac{1}{\rho C_P}\frac{\partial}{\partial \bar{y}}\left(\kappa\frac{\partial T'}{\partial \bar{y}}\right)+\frac{Q_0}{\rho C_P}\left(T'-T'_{\infty}\right)+\frac{\mu}{\rho C_P}\left(\frac{\partial \bar{u}}{\partial \bar{y}}\right)^2+\frac{\sigma {\beta_0}^2}{\rho C_P}\left(\bar{u}\right)^2 \tag{3}$$

Where, $\bar{u}$ and $\bar{v}$ are the velocity components along with the $\bar{x}$ and $\bar{y}$ axis respectively, t' is the time, T' is the temperature of the fluid in the boundary layer and T'_{∞} is the fluid temperature far away from the plate, g is the acceleration due to gravity, κ is the thermal conductivity of the fluid, ρ is the density, C_P is the specific heat at constant pressure and μ is the variable dynamic co-efficient of viscosity of the fluid. The amount of heat generated or absorbed per unit volume is $Q_0\left(T-T_{\infty}\right)$, Q_0 being a constant, which may take either positive or negative and the hydrostatic pressure $\frac{\partial P}{\partial \bar{x}}=-\rho_e g$ where, $\rho_e=\rho$. The source term represents the heat formation when $Q_0>0$ and the heat absorption when $Q_0<0$. $\kappa(T)$ is the thermal conductivity of the fluid depending on the fluid temperature T', σ_0 is the electric conduction and β_0 is the magnetic field strength.

The initial and boundary dimensional conditions are

$$\begin{aligned}
&t'\le 0:\bar{u}=0,\bar{v}=0,T'=T'_{\infty}\text{ for all }\ y\\
&t'>0:\bar{u}=0,\bar{v}=0,T'=T'_{w}\text{ at }\ y=0\\
&t'>0:\bar{u}=0,T'=T'_{\infty}\text{ at }\ x=0\\
&t'>0:\bar{u}=0,T'\to T'_{\infty}\text{ as }\ y\to\infty
\end{aligned} \tag{4}$$

On introducing the following non-dimensional quantities in equations (1) to (4) for programable

$$\begin{aligned}
&x=\frac{\bar{x}}{l},y=\frac{\bar{y}}{l}Gr^{\frac{1}{4}},u=\frac{l\bar{u}}{v}Gr^{\frac{-1}{2}},v=\frac{\bar{v}l}{v}Gr^{\frac{-1}{4}},\\
&t=\frac{vt'}{l^2}Gr^{\frac{1}{2}},T=\frac{T'-T'_{\infty}}{T'_{w}-T'_{\infty}},Gr=\frac{g\beta l^3\left(T'_{w}-T'_{\infty}\right)}{\upsilon^2},\\
&p_r=\frac{\mu_0 C_p}{\kappa_0},\upsilon=\frac{\mu_0}{\rho}
\end{aligned} \tag{5}$$

In this case, *l* stands for plate length, kinematic viscosity, *Gr* for Grashof number, and *Pr* for Prandtl number. The literature has a variety of viscosity and thermal conductivity variations with dimensionless temperature. Stattery [16],

Ockendon and Ockendon [17], El-bashbeshy and Ibrahi [18], and Seddeek and Abdelmegguid [19] have all proposed the following types.

$$\frac{\mu}{\mu_0} = e^{-\lambda T} \tag{6}$$

$$\frac{\kappa}{\kappa_0} = 1 + \gamma T \tag{7}$$

Where λ and γ denote the viscosity and thermal conductivity variation parameters respectively, depended on the nature of the fluid. Here μ_0 and κ_0 are the viscosity and the thermal conductivity at temperature T_w'.

The equation of continuity is

$$\frac{\partial \bar{u}}{\partial \bar{x}} + \frac{\partial \bar{v}}{\partial \bar{y}} = 0$$

$$\Rightarrow \frac{\partial\left(\frac{\upsilon}{l} Gr^{\frac{1}{2}} u\right)}{\partial(xl)} + \frac{\partial\left(\frac{\upsilon}{l} Gr^{\frac{1}{4}} v\right)}{\partial\left(\frac{yl}{Gr^{\frac{1}{4}}}\right)} = 0$$

$$\Rightarrow \frac{\frac{\upsilon}{l} Gr^{\frac{1}{2}}}{l} \frac{\partial u}{\partial x} + \frac{\frac{\upsilon}{l} Gr^{\frac{1}{4}}}{\frac{l}{Gr^{\frac{1}{4}}}} \frac{\partial v}{\partial y} = 0$$

$$\therefore \frac{\partial u}{\partial x} + \frac{\partial v}{\partial y} = 0 \tag{8}$$

Now momentum "EQ" (2) can be reduced by applying the non- dimensional transformation "EQ" (5) and "EQ" (6), we have

$$\frac{\partial \bar{u}}{\partial t'} + \bar{u}\frac{\partial \bar{u}}{\partial \bar{x}} + \bar{v}\frac{\partial \bar{u}}{\partial \bar{y}} = \frac{1}{\rho}\frac{\partial}{\partial \bar{y}}\left(\mu \frac{\partial \bar{u}}{\partial \bar{y}}\right) + g\beta\left(T' - T_\infty'\right)$$

$$\Rightarrow \frac{Gr\upsilon^2}{l^3}\frac{\partial u}{\partial t} + \frac{Gr\upsilon^2}{l^3} u\frac{\partial u}{\partial x} + \frac{Gr\upsilon^2}{l^3} v\frac{\partial u}{\partial y}$$

$$= \frac{1}{\rho}\frac{\upsilon Gr \mu_0}{l^3}\frac{\partial}{\partial y}\left(e^{-\lambda T}\frac{\partial u}{\partial y}\right) + g\beta\left(T_w' - T_\infty'\right)$$

$$\Rightarrow \frac{\partial u}{\partial t} + u\frac{\partial u}{\partial x} + v\frac{\partial u}{\partial y} = \left[e^{-\lambda T}\frac{\partial^2 u}{\partial y^2} - \lambda e^{-\lambda T}\frac{\partial T}{\partial y}\frac{\partial u}{\partial y}\right] + T \tag{9}$$

Again, the energy "EQ" (3) can be reduced by the above similarity transformation "EQ" (5) and "EQ" (7), we have

$$\Rightarrow \frac{\partial T'}{\partial t'} + \bar{u}\frac{\partial T'}{\partial \bar{x}} + \bar{v}\frac{\partial T'}{\partial \bar{y}} = \frac{1}{\rho C_P}\frac{\partial}{\partial \bar{y}}\left(\kappa \frac{\partial T'}{\partial \bar{y}}\right) + \frac{Q_0}{\rho C_P}\left(T' - T_\infty'\right) + \frac{\mu}{\rho C_P}\left(\frac{\partial \bar{u}}{\partial y}\right)^2$$

$$+ \frac{\sigma {\beta_0}^2}{\rho C_P}(\bar{u})^2$$

$$\frac{\partial\{T_\infty' + T(T_w' - T_\infty')\}}{\partial\left(tl^2 \Big/ \upsilon Gr^{\frac{1}{2}}\right)} + \frac{\upsilon u}{l} Gr^{\frac{1}{2}} \frac{\partial\{T_\infty' + T(T_w' - T_\infty')\}}{\partial(xl)} + \frac{\upsilon v}{l} Gr^{\frac{1}{4}} \frac{\partial\{T_\infty' + T(T_w' - T_\infty')\}}{\partial\left(yl \Big/ Gr^{\frac{1}{4}}\right)}$$

$$\Rightarrow \frac{1}{\rho C_p}\frac{\partial}{\partial\left(yl \Big/ Gr^{\frac{1}{2}}\right)}\left(\kappa \frac{\partial\left\{T_\infty' + T\left(T_w' - T_\infty'\right)\right\}}{\partial\left(yl \Big/ Gr^{1/4}\right)}\right) + \frac{Q_0}{\rho C_p}\left(T' - T_\infty'\right) + \frac{\mu}{\rho C_p}\left(\frac{\partial\left(\upsilon u Gr^{\frac{1}{2}} \Big/ l\right)}{\partial\left(yl \Big/ Gr^{\frac{1}{2}}\right)}\right)^2$$

$$+ \frac{\sigma {\beta_0}^2}{\rho C_p}\left(\frac{u^2\upsilon^2}{l^2} Gr\right)\frac{\upsilon Gr^{\frac{1}{2}}\left(T_w' - T_\infty'\right)}{l^2}\frac{\partial T}{\partial t}$$

$$+ \frac{\upsilon Gr^{\frac{1}{2}}\left(T_w' - T_\infty'\right)}{l^2} u\frac{\partial T}{\partial x} + \frac{\upsilon Gr^{\frac{1}{2}}\left(T_w' - T_\infty'\right)}{l^2} v\frac{\partial T}{\partial y}$$

$$= \frac{Gr^{\frac{1}{2}}\left(T_w' - T_\infty'\right)}{l^2 \rho C_p}\frac{\partial}{\partial y}\left\{\kappa_0\left(1 + \gamma T\right)\frac{\partial T}{\partial y}\right\} + \frac{Q_0}{\rho C_P}\left(T' - T_\infty'\right)$$

$$+ \frac{\mu}{\rho C_P}\frac{\upsilon^2 Gr Gr^{\frac{1}{2}}\left(T_w' - T_\infty'\right)}{l^2 l^2}\left(\frac{\partial u}{\partial y}\right)^2 + \frac{\sigma {\beta_0}^2 \upsilon^2 Gr}{\rho C_p l^2} u^2$$

$$\Rightarrow \frac{\partial T}{\partial t}+u\frac{\partial T}{\partial x}+v\frac{\partial T}{\partial y}=\frac{\kappa_0}{\mu_0 C_p}\left\{\left(1+\gamma T\right)\frac{\partial^2 T}{\partial y^2}+\gamma\left(\frac{\partial T}{\partial y}\right)^2\right\}+$$

$$\frac{Q_0 l^2\left(T'-T'_\infty\right)}{\rho C_P \upsilon Gr^{1/2}\left(T'_w-T'\right)}+$$

$$\frac{\mu\upsilon^2 Gr^{3/2}}{\rho C_P l^4}\left(\frac{\partial u}{\partial y}\right)^2\frac{l^2}{\upsilon Gr^{1/2}\left(T'_w-T'_\infty\right)}+\frac{\sigma{\beta_0}^2\upsilon^2 Gr}{\rho C_P l^2}u^2\frac{l^2}{\upsilon Gr^{1/2}\left(T'_w-T'_\infty\right)}$$

$$\Rightarrow \frac{\partial T}{\partial t}+u\frac{\partial T}{\partial x}+v\frac{\partial T}{\partial y}=\frac{1}{p_r}\left\{\left(1+\gamma T\right)\frac{\partial^2 T}{\partial y^2}+\gamma\left(\frac{\partial T}{\partial y}\right)^2\right\}$$

$$+\frac{Q_0 l^2\left(T'-T'_\infty\right)}{\rho C_P \upsilon Gr^{1/2}\left(T'_w-T'\right)}+\frac{\mu\upsilon Gr}{\rho C_P l^2\left(T'_w-T'_\infty\right)}\left(\frac{\partial u}{\partial y}\right)^2$$

$$+\frac{\sigma{\beta_0}^2\upsilon^2 Gr}{\rho C_P \upsilon Gr^{1/2}\left(T'_w-T'_\infty\right)}u^2$$

$$\Rightarrow \frac{\partial T}{\partial t}+u\frac{\partial T}{\partial x}+v\frac{\partial T}{\partial y}=\frac{1}{P_r}\left[\gamma\left(\frac{\partial T}{\partial u}\right)^2\right]$$

$$+\frac{1}{P_r}\left[\left(1+\gamma T\right)\frac{\partial^2 T}{\partial y^2}\right]+QT+\frac{\mu\upsilon g\beta l^3}{\rho C_P l^2\left(T'_w-T'_\infty\right)\upsilon^2}\left(T'_w-T'_\infty\right)\left(\frac{\partial u}{\partial y}\right)^2$$

$$+\frac{\sigma{\beta_0}^2\upsilon Gr^{1/2}}{\rho C_P\left(T'_w-T'_\infty\right)}u^2$$

$$\Rightarrow \frac{\partial T}{\partial t}+u\frac{\partial T}{\partial x}+v\frac{\partial T}{\partial y}=\frac{1}{P_r}\left[\gamma\left(\frac{\partial T}{\partial y}\right)^2\right]+\frac{1}{P_r}\left[\left(1+\gamma T\right)\frac{\partial^2 T}{\partial y^2}\right]+QT+$$

$$\frac{\mu g\beta l}{\rho C_P\upsilon}\left(\frac{\partial u}{\partial y}\right)^2+\frac{\sigma{\beta_0}^2\upsilon Gr^{1/2}}{\rho C_P\left(T'_w-T'_\infty\right)}u^2$$

$$\Rightarrow \frac{\partial T}{\partial t}+u\frac{\partial T}{\partial x}+v\frac{\partial T}{\partial y}=\frac{1}{P_r}\left[\gamma\left(\frac{\partial T}{\partial u}\right)^2\right]+\frac{1}{P_r}\left[\left(1+\gamma T\right)\frac{\partial^2 T}{\partial y^2}\right]+QT$$

$$+\frac{\mu g\beta l}{\rho C_P\frac{\mu}{\rho}}\left(\frac{\partial u}{\partial y}\right)^2+\frac{\sigma{\beta_0}^2\upsilon Gr^{1/2}}{\rho C_P\left(T'_w-T'_\infty\right)}u^2$$

$$\Rightarrow \frac{\partial T}{\partial t}+u\frac{\partial T}{\partial x}+v\frac{\partial T}{\partial y}=\frac{1}{P_r}\left[\gamma\left(\frac{\partial T}{\partial u}\right)^2\right]+\frac{1}{P_r}\left[\left(1+\gamma T\right)\frac{\partial^2 T}{\partial y^2}\right]+QT$$

$$+\frac{g\beta l}{C_P}\left(\frac{\partial u}{\partial y}\right)^2+\frac{\sigma{\beta_0}^2\upsilon Gr^{1/2}}{\rho C_P\left(T'_w-T'_\infty\right)}u^2$$

$$\Rightarrow \frac{\partial T}{\partial t}+u\frac{\partial T}{\partial x}+v\frac{\partial T}{\partial y}=$$

$$\frac{1}{P_r}\left[\gamma\left(\frac{\partial T}{\partial u}\right)^2\right]+\frac{1}{P_r}\left[\left(1+\gamma T\right)\frac{\partial^2 T}{\partial y^2}\right]+QT+N\left(\frac{\partial u}{\partial y}\right)^2+Jul\left(u^2\right) \tag{10}$$

The corresponding initial conditions and boundary conditions in a non-dimension form are as follows

$$\begin{aligned} &t \le 0 : u = 0, v = 0, \mathrm{T} = 0, \text{ for all } y \\ &t > 0 : u = 0, v = 0, \mathrm{T} = 1, \text{ at } y = 0 \\ &u = 0, \mathrm{T} = 0 \text{ at } x = 0 \\ &u \to 0, \mathrm{T} \to 0 \text{ at } y \to \infty \end{aligned} \tag{11}$$

u, v are the velocity components along with *x* and *y* axis respectfully *t* is time, *T* is the temperature.

"EQ" (4) indicates initial and boundary conditions (dimensional) and "EQ" (11) indicates initial and boundary conditions (dimensionless).

The free convective unstable laminar boundary layer flow with variable viscosity and thermal conductivity and an isothermal semi-infinite vertical plate is described by "EQ" (8) to "EQ" (10) with the boundary condition "EQ" (11).

Where, $p_r = \mu_0 C_P / \kappa_0$, the Prandtl's number, $Q_0 l^2 / \mu C_P G r^{1/2} = Q$ is the heat formation parameter $Jul = \dfrac{\sigma \beta_0^2 \upsilon G r^{1/2}}{\rho C_P (T_w' - T_\infty')}$, is the joule heating parameter and $N = g\beta l / C_P$ is viscous dissipation parameter.

The local shear stress in the plate is defined by

$$\tau_{\bar{x}} = \left(\mu \frac{\partial \bar{u}}{\partial \bar{y}} \right)_{\bar{y}=0} \tag{12}$$

The non-dimensional form of local skin friction, which is obtained by introducing the non-dimensional quantities found in "EQ" (5) – "EQ" (6) in "EQ" (12), is provided by

$$\begin{aligned} &\tau_{\bar{x}} = \left(\mu \frac{\partial \bar{u}}{\partial \bar{y}} \right)_{\bar{y}=0} \\ &\Rightarrow \frac{l^2}{\upsilon \mu_0} \tau_{(xl)} = G r^{3/4} e^{-\lambda} \left[\frac{\partial u}{\partial y} \right]_{y=0} \\ &\therefore \bar{\tau}_x = G r^{3/4} e^{-\lambda} \left[\frac{\partial u}{\partial y} \right]_{y=0} \end{aligned} \tag{13}$$

The integration of "EQ" (13) from $x = 0$ to gives $x = 1$ the average skin friction and it is given by

$$\therefore \bar{\tau} = e^{-\lambda} G r^{3/4} \int_0^1 \left(\frac{\partial u}{\partial y} \right)_{y=0} dx \tag{14}$$

The local Nusselt number is defined by

$$\begin{aligned} &N_{u_{\bar{x}}} = \frac{-l \left(\kappa \dfrac{\partial T'}{\partial \bar{y}} \right)_{\bar{y}=0}}{\kappa_0 (T_w' - T_\infty')} \\ &\Rightarrow N_{u_{(xl)}} = -l \left[\frac{\kappa_0 (1 + \gamma T)}{\kappa_0 (T_w' - T_\infty') l G r^{\frac{-1}{4}}} \left(\frac{\partial T}{\partial y} \right)_{y=0} \right] \\ &\Rightarrow G r^{-1/4} (T_w' - T_\infty') N_{u_{(xl)}} = -(1+\gamma) \left(\frac{\partial T}{\partial y} \right)_{y=0} \quad \because y = 0, T = 1 \\ &\Rightarrow \bar{N}_{u_x} = -(1+\gamma) \left(\frac{\partial T}{\partial y} \right)_{x=0} \\ &\therefore \bar{N}_{u_x} = -(1+\gamma) \left(\frac{\partial T}{\partial y} \right)_{y=0} \\ &\therefore \bar{N}_{u_x} = -(1+\gamma) \left(\frac{\partial T}{\partial y} \right)_{y=0} \end{aligned} \tag{15}$$

The integration of "EQ" (15) from *x=0* to *x=1* gives the average skin friction and it is given by

$$\therefore \bar{N}_{u_x} = -(1+\gamma) \int_0^1 \left(\frac{\partial T}{\partial y} \right)_{y=0} dx \tag{16}$$

3. Numerical Techniques

There are many advanced numerical methods like finite difference method, Keller box method, Runge- Kutta shooting method, Spectral collocation method, Finite element method. The two-dimensional, non-linear, unsteady and coupled partial differential "EQ" (8), "EQ" (10) under the initial and boundary conditions in "EQ" (11) are solved using an implicit finite difference scheme of Crank-Nicolson type which is the fast convergent and unconditionally stable. The finite difference equation corresponding to the "EQ" (8) to "EQ" (10) are given by

$$\begin{aligned} &\frac{\left[u_{i,j}^{k+1} - u_{i-1,j}^{k+1} + u_{i,j}^{k} - u_{i-1,j}^{k} + u_{i,j-1}^{k+1} - u_{i-1,j-1}^{k+1} + u_{i,j-1}^{k} - u_{i-1,j-1}^{k} \right]}{4\Delta x} \\ &+ \frac{\left[v_{i,j}^{k+1} - v_{i,j-1}^{k+1} + v_{i,j}^{k} - v_{i,j-1}^{k} \right]}{2\Delta y} = 0 \end{aligned} \tag{17}$$

$$\frac{\left[u_{i,j}^{k+1}-u_{i,j}^{k+1}\right]}{2\Delta t}+u_{i,j}^{k}\frac{\left[u_{i,j}^{k+1}-u_{i-1,j}^{k+1}+u_{i,j}^{k}-u_{i-1,j}^{k}\right]}{2\Delta x}$$
$$v_{i,j}^{k}\frac{\left[u_{i,j+1}^{k+1}-u_{i,j-1}^{k+1}+u_{i,j+1}^{k}-u_{i,j-1}^{k}\right]}{4\Delta y}=\frac{1}{2}\left[T_{i,j}^{k+1}+T_{i,j}^{k}\right]+e^{-\lambda}\left[\frac{T_{i,j}^{k+1}+T_{i,j}^{k}}{2}\right]$$
$$\frac{\left[u_{i,j-1}^{k+1}-2u_{i,j}^{k+1}+u_{i,j+1}^{k}+u_{i,j-1}^{k}-2u_{i,j}^{k}+u_{i,j+1}^{k}\right]}{2(\Delta y)^{2}}$$
$$-\lambda e^{-\lambda}\left[\frac{T_{i,j}^{k+1}+T_{i,j}^{k}}{2}\right]\frac{\left[T_{i,j+1}^{k+1}-T_{i,j-1}^{k+1}+T_{i,j+1}^{k}-T_{i,j-1}^{k}\right]}{4\Delta y} \tag{18}$$
$$\frac{\left[u_{i,j+1}^{k+1}-u_{i,j-1}^{k+1}+u_{i,j+1}^{k}-u_{i,j-1}^{k}\right]}{4\Delta y}\left[\frac{T_{i,j}^{k+1}-T_{i,j}^{k}}{2\Delta t}\right]+u_{i,j}^{k}\frac{\left[T_{i,j}^{k+1}-T_{i-1,j}^{k+1}+T_{i,j}^{k}-T_{i-1,j}^{k}\right]}{4\Delta x}$$
$$+v_{i,j}^{k}\frac{\left[T_{i,j-1}^{k+1}-T_{i,j-1}^{k+1}+T_{i,j+1}^{k}-T_{i,j-1}^{k}\right]}{4\Delta y}$$
$$=\frac{1+\gamma T_{i,j}^{k}}{p_r}\frac{\left[T_{i,j-1}^{k+1}-2T_{i,j}^{k+1}+T_{i,j+1}^{k}+T_{i,j-1}^{k}-2T_{i,j}^{k}+T_{i,j+1}^{k}\right]}{2(\Delta y)^{2}}$$
$$\frac{\gamma}{p_r}\left[\frac{\left[T_{i,j+1}^{k+1}-T_{i,j-1}^{k+1}+T_{i,j+1}^{k}-T_{i,j-1}^{k}\right]}{4\Delta y}\right]+\frac{Q}{2}\left[T_{i,j}^{k+1}+T_{i,j}^{k}\right]+Jul\left\{\frac{1}{2}\left[u_{i,j}^{k+1}+u_{i,j}^{k}\right]\right\}^{2} \tag{19}$$
$$+N\left\{\frac{\left[u_{i,j+1}^{k+1}-u_{i,j-1}^{k+1}+u_{i,j+1}^{k}-u_{i,j-1}^{k}\right]}{4\Delta y}\right\}^{2}$$

The region of integration is considerably outside the momentum and energy boundary layers and is represented by a rectangle with sides $x_{\max}$ *(=1)* and $y_{\max}$ *(=10),* where $y_{\max}$ corresponds to *y* approaches to ∞. The maximum of *y* was chosen as 6 after some preliminary investigations so that the last two of the boundary conditions (11) are satisfied. In this case, the grid point along the *u*-direction is indicated by the subscript *i*, the *v*-direction by *j*, and the *t*-direction by the superscript *k*. The coefficients $u_{i,j}^{k}$ and $v_{i,j}^{k}$ that appear in the difference equations are treated as constants throughout any one-time step.

Because of the beginning conditions, we know the values of *u*, *v*, and *T* at every grid point at *t = 0.* The following is how the data from the previous time level (fe) are used to calculate *u*, *v*, and *T* at time level *(k + 1):* The tridiagonal system of equations is made up of the finite difference "EQ" (18) at each internal nodal point on a specific i-level. According to Carnahan et al. [19], the Thomas method solves such a system of equations. For a given i at the *(k + l) t*h time level, the values of *T* are therefore determined at each nodal point.

The values of *u* at *(k + 1)* th time level are found similarly to the values of *T* at *(k + 1)* th time level in "EQ" (13). Consequently, on a specific i-level, the values of *T* and *u* are known. Lastly, at each nodal point on a certain *i*-level at *(k + 1)* th time level, the values of *v* are explicitly determined using the "EQ" (12). For different i-levels, this procedure is repeated. Thus, at the *(k + 1)* th time level, the values of *T*, *u*, and *v* are known at every grid point in the rectangular region.

They have been fixed at the level $\Delta x = 0.05$, $\Delta y = 0.25$, and time step $\Delta t = 0.01$ after a few sets of mesh sizes were taken into consideration. The results are compared after the spatial mesh size is reduced by 50% in one direction and subsequently in both directions. It has been noted that the results vary to the fourth decimal place when the mesh size is decreased by 50% in both the *x* and *y* directions. As a result, the sizes listed above have been deemed suitable for calculations.

Until the steady-state is achieved, calculations are made. When the absolute difference between the values of *u* and temperature *T* at two consecutive time steps is smaller than 10^{-5} at all grid points, the steady-state solution is said to have been reached.

The local truncation error is $O(\Delta f^2 + \Delta F^2 + \Delta Ax)$ and it $\rightarrow 0$ as $\Delta t. \Delta x$ and $\Delta y \rightarrow 0$, which shows that the scheme is compatible. Additionally, it is demonstrated that the Crank-Nicolson type of implicit finite difference scheme is

unconditionally stable for a natural convective flow, where the velocity u and v are always non-negative and non-positive, respectively. Therefore, the implicit finite difference scheme's convergence is guaranteed by compatibility and stability.

4. Results and Discussion

Heat conduction, also known as thermal diffusion, refers to the microscopic transfer of kinetic energy between particles across a temperature gradient. Among conventional fluids, water is widely used in thermal systems due to its high specific heat capacity and low viscosity, which facilitate efficient heat transport. In certain applications, oil is preferred over water because of its higher boiling point, which enables operation at elevated temperatures without the complications associated with high pressure.

Heat transfer mechanisms can generally be categorized into three modes: conduction, convection, and radiation. Convection involves the bulk movement of fluid—such as air or water—carrying thermal energy from one region to another, typically driven by temperature-induced density gradients. For instance, when air is heated, it expands, becomes less dense, and rises, thereby transporting heat through natural convection. Even in fully developed turbulent flows, thermal conduction at the molecular level remains significant, particularly in the near-wall region and within the core of the flow, especially for low-Prandtl-number fluids such as liquid metals.

The following ranges for λ, γ and Pr are considered in the present study are:

For air: $-0.7 \le \lambda \le 0$, $0 \le \gamma \le 6$, $Pr = 0.733$

For water: $0 \le \lambda \le 0.6$, $0 \le \gamma \le 0.12$, $2 \le Pr \le 7.00$

To assess the precision of our calculated values, we plot the curves calculated by G. palani, Kwang-Yong Kim, and Elbashbeshy & Ibrahim for different values of λ and γ for air *(Pr = 0.733)* in Figure 2 and Figure 3. Our results show excellent agreement with those of G. palani, Kwang-Yong Kim, and Elbashbeshy & Ibrahim at the steady state.

The body force hasn't had enough time to create the proper motion in the fluid during the first phase of the subsequent step changes in the wall temperature. For short times t, the velocity components u and v are therefore insignificant. For constant viscosity and thermal conductivity, pure heat conduction dominates the heat transfer throughout this first transient period. The result of "EQ" (10) is

$$\frac{\partial u}{\partial T} = \frac{1}{pr}\frac{\partial^2 T}{\partial y^2}$$

For brief periods, it is seen that the temperature profile depends solely on time and the normal distance from the wall for a given Prandtl's number. Under the beginning and boundary conditions specified in the local Nusellt number, the solutions of "EQ" (15) with $Pr = 1$ are

$$T = erfc\left(\frac{y}{2\sqrt{t}}\right) \qquad (20)$$

Figure 4 and Figure 5, Figure 6 and Figure 7, Figure 8 and Figure 9, Figure 10 and Figure 11, Figure 12 and Figure 13, Figure 14 and Figure 15, Figure 16 and Figure 17 show that the variation of velocity and temperature at their transient, temporal maximum and steady state against the co-ordinate y at the leading edge of the plate viz., $x = 1.0$ for variable viscosity, thermal conductivity, heat conduction variation parameters, pressure work parameters and Prandtl's numbers. The fluid velocity increases and reached its maximum value at very near to the wall (i.e., $0 \le y \le 8$) and then decreases monotonically to zero as y becomes large for all time t. It is also observed that the velocity and temperature increase with time t, reaches a temporal maximum and consequently it reaches the steady state.

Figure 4 and Figure 5 how that the variation of transient velocity and temperature profiles with area A. for a fixed value of $\gamma = 0.10$, $Pr = 0.73$, $Q = 0.50$, $N = 0.75$, $Jul=0.80$ From "Figure 4" he velocity of the fluid increases with time till a transient maximum is reached and then a moderate reduction is mentioned till the alternate balanced condition is reached. It is mentioned that the time taken to goes the steady condition reduces hardly at all with a raising the viscosity variation parameter. From Figure 4 it is obvious that velocity u at any vertical plane near to the plate increases as variable viscosity λ decrease. But after certain time the velocity profile twisted an opposite trend. And finally it meets with y axis asymptotically. From Figure 5 it is mentioned that the temperature of the fluid reduces as λ raises. It is also related for different time.

The numerical values of the variation of transient velocity and temperature for the fixed value of $\lambda = 0.30$, $Q = 0.50$, $N = 0.75$ $Pr = 0.73$ and $Jul=0.80$ with the variation of thermal conductivity parameter γ are shown graphically in Figure 6 and Figure 7 from these figures, it is observed that the velocity and temperature distribution in the fluid increases as γ increases for fixed value of λ, Q, N, Jul heating and Prandtl's number. It can also be noticed that with an increase in γ, the rise in the magnitude of the velocity and temperature is significant, which implies that the volume flow rate increases with an increase in γ. The effects of variation of thermal conductivity on velocity and temperature is more important even in the initial transient timing. Also, it is observed that the time to reach the temporal maximum and steady state decreases with increasing thermal conductivity parameter γ.

The numerical values of variation velocity and temperatures are computed from "EQ" (13) and "EQ" (14) are depicted in the graphical form in the Figure 8 and Figure 9 for different values of N for fixed value of $Q = 0.50$, Jul=0.80, $\gamma = 0.10$ in water ($Pr = 0.70$) and $\lambda=0.30$. It is clearly mentioned that the taken time to reach the temporal extreme and balanced state reduces with decreasing the values of Jul. It can be represented from Figure 8 it is obvious that the velocity u at any vertical plane near to the plate increases as parameter viscous dissipation increases. But after a certain time the velocity profile twisted an opposite trend. And finally it meets asymptotically.

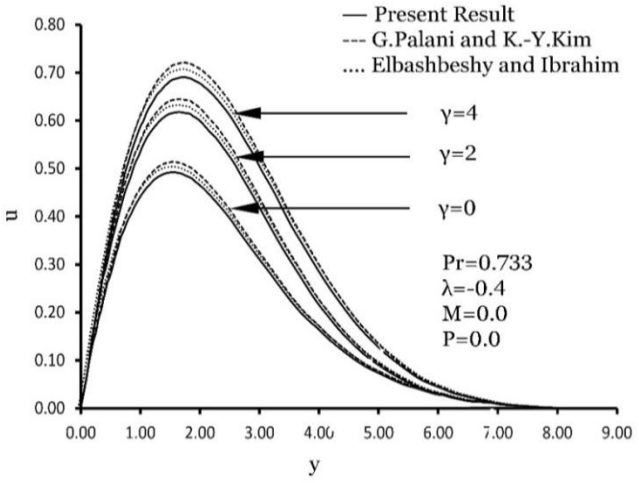

Figure 2. Comparison of Velocity profiles G. Palani and K.-Y. Kim. Elbashbeshy and Ibrahim for various values

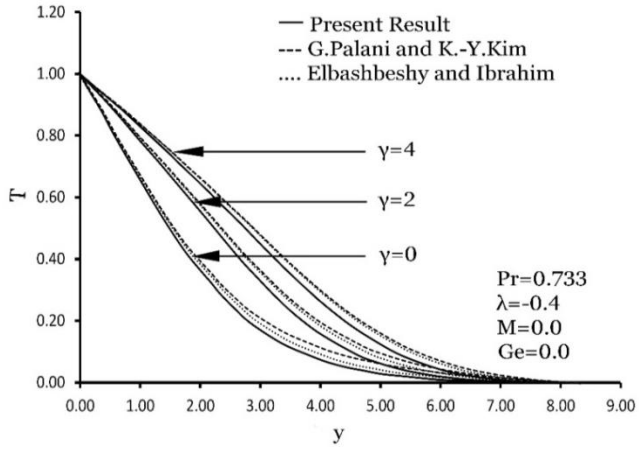

Figure 3. Comparison of Temperature profiles G. Palani and K.-Y. Kim. Elbashbeshy and Ibrahim for various values

Figure 2 and Figure 3 Comparison of velocity profiles and temperature profiles G. Palani and K.-Y. Kim. Elbashbeshy and Ibrahim for various values of dependent thermal conductivity with fixed values.

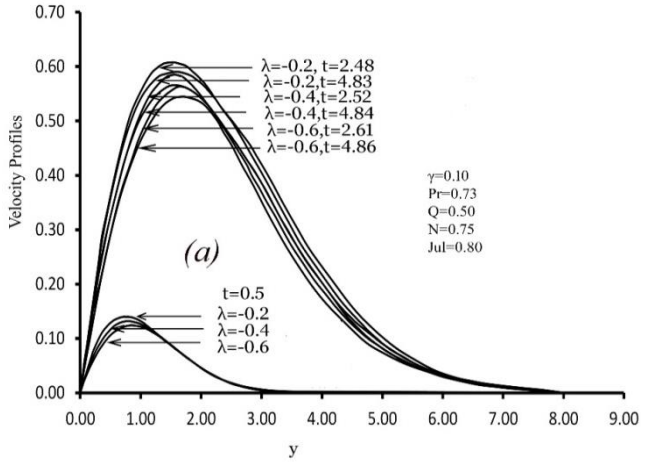

Figure 4. Variation of dimensionless Velocity profiles versus dimensionless y for various values of viscosity λ and steady state condition with Q=0.5, N=0.75, Jul=0.8, γ=0.1 and Pr= 0.73

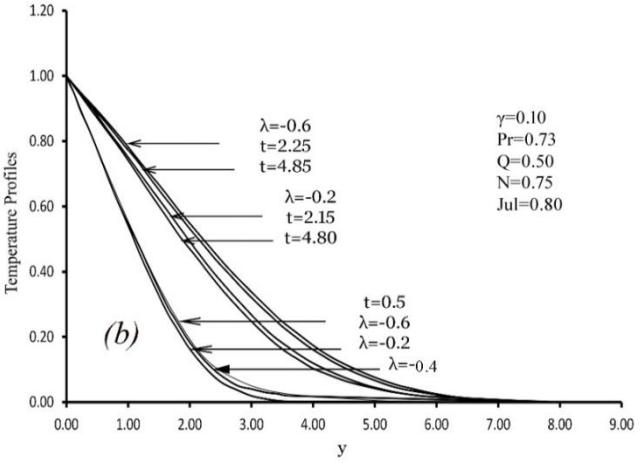

Figure 5. Variation of dimensionless Temperature profiles versus dimensionless y for various values of viscosity λ and steady state condition with Q=0.5, N=0.75, Jul=0.8, γ=0.1 and Pr= 0.73

Figure 4 and Figure 5 Variation of dimensionless velocity and temperature profiles versus dimensionless *y* for various values of viscosity λ and steady state condition with *Q=0.5, N=0.75, Jul=0.8,* γ *=0.1* and *Pr= 0.73.*

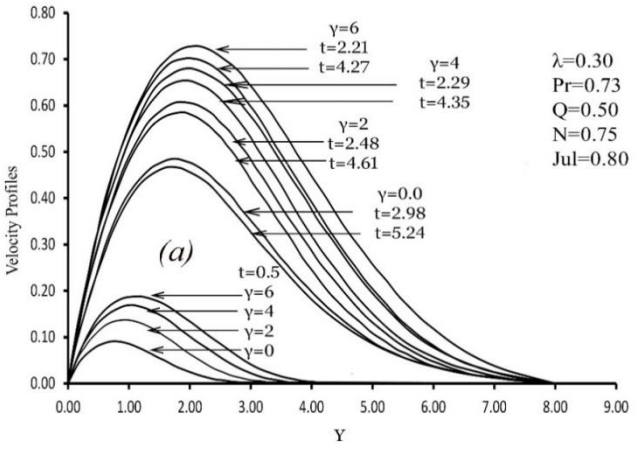

Figure 6. Variation of dimensionless Velocity profiles versus dimensionless y for various values of thermal conductivity γ and steady state condition with Q=0.5, N=0.75, Jul=0.8, λ =0.30 and Pr= 0.73

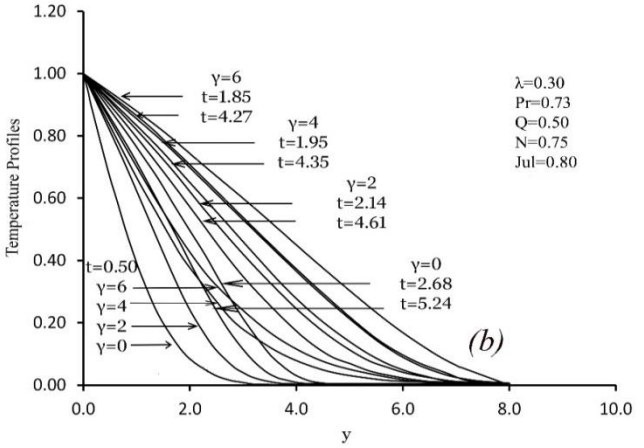

Figure 7. Variation of dimensionless velocity and temperature profiles versus dimensionless y for various values of thermal conductivity λ and steady state condition with Q=0.5, N=0.75, Jul=0.8, λ =0.30 and Pr= 0.73

Figure 6 and Figure 7 Variation of dimensionless velocity and temperature profiles versus dimensionless *y* for various values of thermal conductivity γ and steady state condition with *Q=0.5, N=0.75, Jul=0.8,* λ *=0.30* and *Pr= 0.73.*

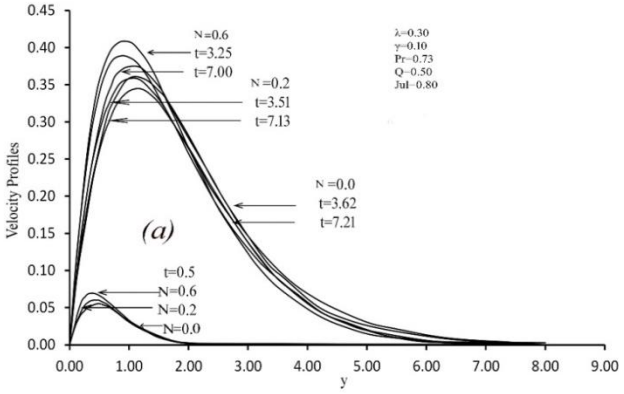

Figure 8. Variation of dimensionless velocity and temperature profiles versus dimensionless y for different values of viscous dissipation N and steady state condition with Q=0.5, γ=0.10, Jul=0.8, λ =0.30 and Pr= 0.73

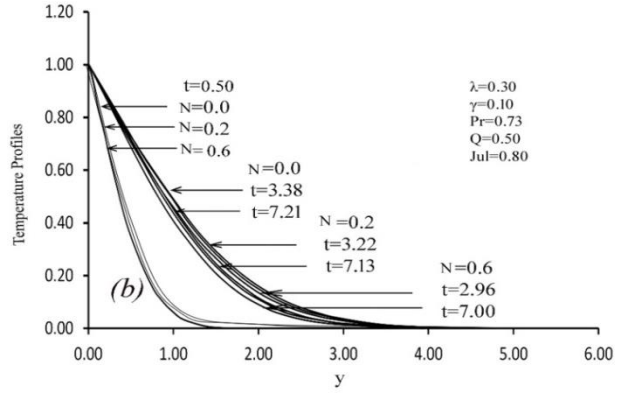

Figure 9. Variation of dimensionless velocity and temperature profiles versus dimensionless y for different values of viscous dissipation N and steady state condition with Q=0.5, γ=0.10, Jul=0.8, λ =0.30 and Pr= 0.73

Figure 8 and Figure 9 Variation of dimensionless velocity and temperature profiles versus dimensionless *y* for different values of viscous dissipation *N* and steady state condition with *Q=0.5,* γ *=0.10, Jul=0.8,* λ *=0.30* and *Pr= 0.73.*

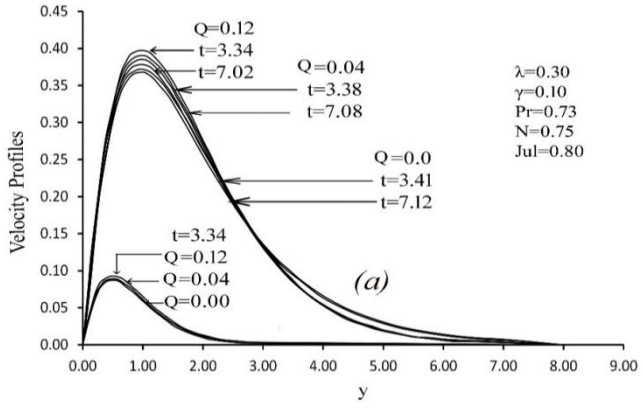

Figure 10. Variation of dimensionless Velocity profiles versus dimensionless y for different values of heat generation Q and steady state condition with N=0.75, γ=0.10, Jul=0.8, λ =0.30 and Pr= 0.73

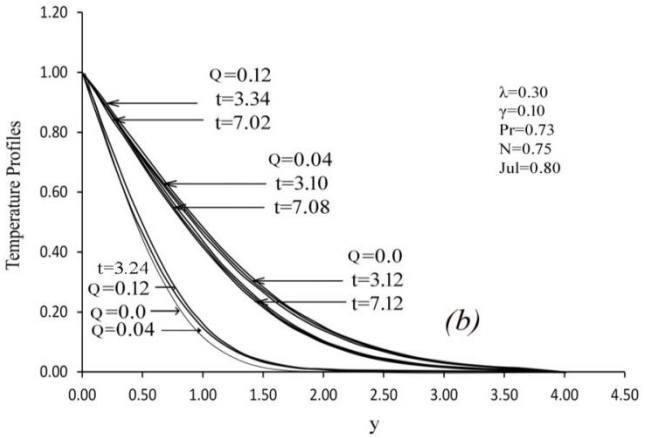

Figure 11. Variation of dimensionless velocity and temperature profiles versus dimensionless y for different values of heat generation Q and steady state condition with N=0.75, γ=0.10, Jul=0.8, λ =0.30 and Pr= 0.73

Figure 10 and Figure 11 Variation of dimensionless velocity and temperature profiles versus dimensionless *y* for different values of heat generation *Q* and steady state condition with *N=0.75,* γ *=0.10, Jul=0.8,* λ *=0.30* and *Pr= 0.73.*

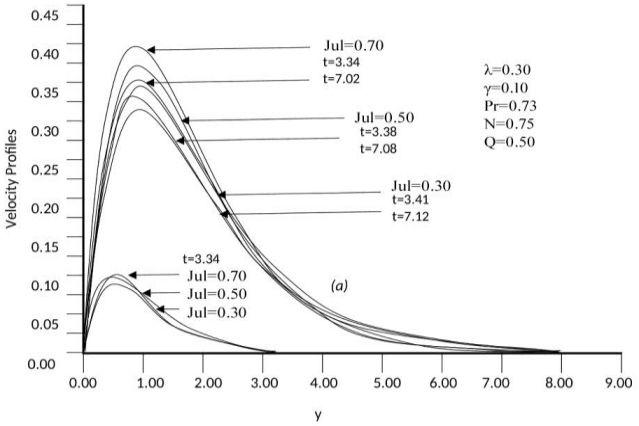

Figure 12. Variation of dimensionless Velocity profiles versus dimensionless y for different values of Joule and steady state condition with N=0.75, γ=0.10, Q=0.50, λ =0.30 and Pr= 0.73

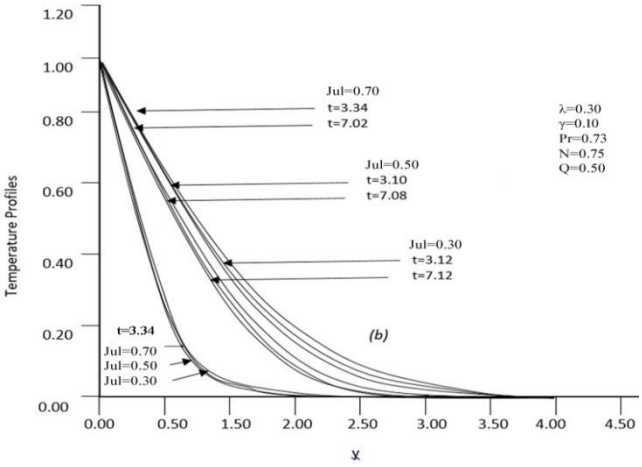

Figure 13. Variation of dimensionless Temperature profiles versus dimensionless y for different values of Joule and steady state condition with N=0.75, γ=0.10, Q=0.50, λ =0.30 and Pr= 0.73

Figure 12 and Figure 13 Variation of dimensionless velocity and temperature profiles versus dimensionless *y* for different values of Joule and steady state condition with *N= 0.75, γ = 0.10, Q=0.50, λ =0.30* and *Pr = 0.73.*

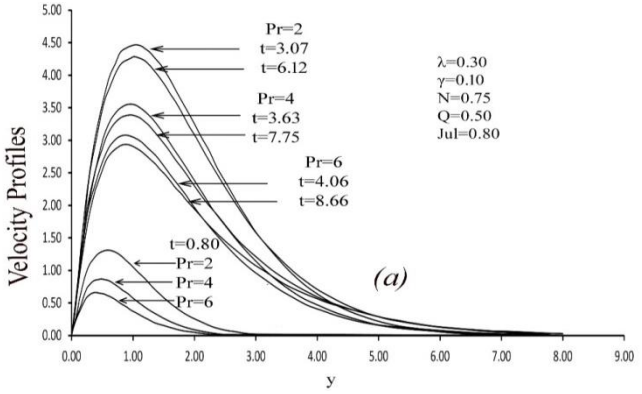

Figure 14. Variation of dimensionless Velocity profiles against dimensionless y for different values of prandtl's number Pr and steady state condition with N=0.75, γ=0.10, Q=0.5, λ =0.30 and Jul= 0.80

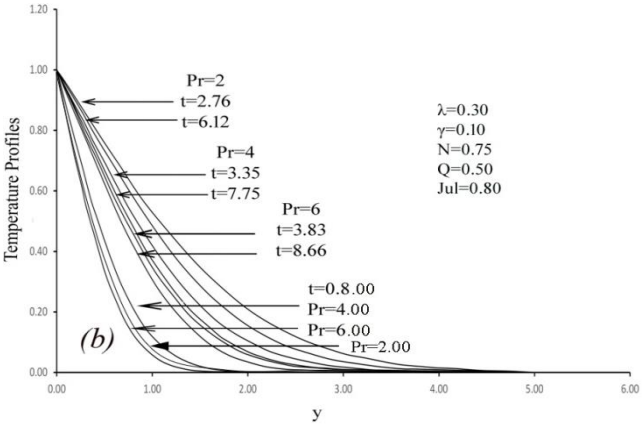

Figure 15. Variation of dimensionless Temperature profiles against dimensionless y for different values of prandtl's number Pr and steady state condition with N=0.75, γ=0.10, Q=0.5, λ =0.30 and Jul= 0.80

Figure 14 and Figure 15 Variation of dimensionless velocity and temperature profiles against dimensionless *y* for different values of prandtl's number *Pr* and steady state condition with *N = 0.75, γ = 0.10, Q = 0.5, λ = 0.30* and *Jul = 0.80.*

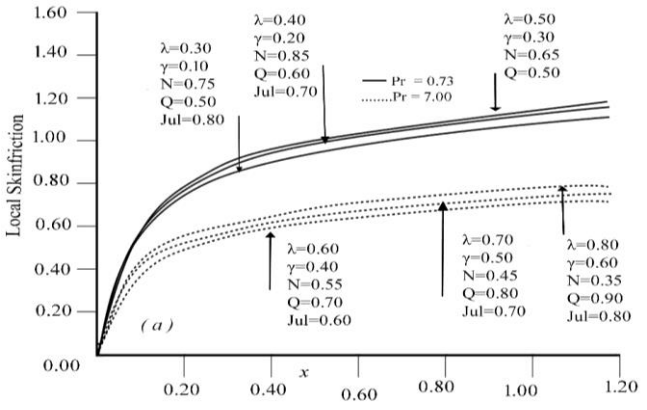

Figure 16. Variation of dimensionless Local Skin Friction versus dimensionless distance x for different values of Q, λ, γ, N, Jul and Pr at steady state condition

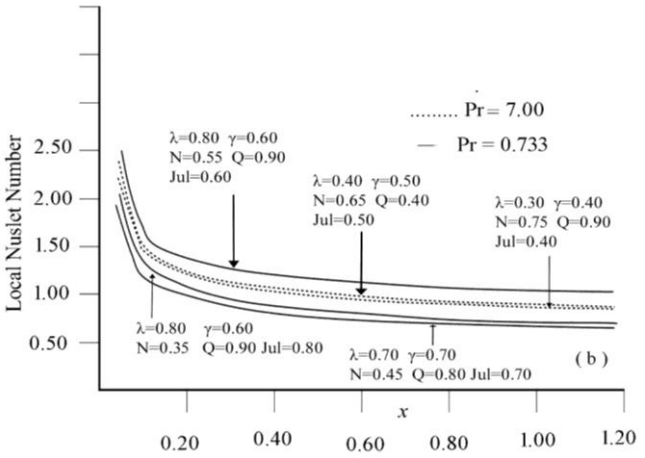

Figure 17. Variation of dimensionless Local Nusselt number versus dimensionless distance x for different values of Q, λ, γ, N, Jul and Pr at steady state condition

Figure 16 and Figure 17 Variation of dimensionless local skin friction and local Nusselt number versus dimensionless distance *x* for different values of *Q, λ, γ, N, Jul* and *Pr* at steady state condition.

From Figure 9, it is mentioned that the temperature of the fluid decreases as the parameter of viscous dissipation increases. It is also related for different time.

Figure 10 and Figure 11 show that the variation of velocity and temperature for various values of heat generation *Q* for fixed value of *λ = 0.30, γ =0.10, N = 0.75, Jul=0.80* in air *(Pr = 0.73).* It is clearly mentioned that the taken time to reach the temporal extreme and balanced state reduces with decreasing the values of heat generation *Q*. It can be represented from Figure 10 it is obvious that the velocity *u* at any vertical plane near to the plate increases as parameter heat generation *Q* increases. But after a certain time, the velocity profile twisted an opposite trend. And finally, it meets asymptotically. From Figure 11 it is mentioned that the temperature of the fluid decreases as the parameter heat generation *Q* increases. It is also related for different time.

The variation of transient velocity and temperature with *Joule* heating for fixed values *Pr = 0.73, λ = 0.30, Q = 0.50, N=0.75* and *γ = 0.10* are shown in Figure 12 and Figure 13. It is observed that the time taken to reach the temporal maximum and steady state increases with the increasing value of *Joule* heating parameter *Jul* of the fluid. From the numerical results, we observe that the velocity profile increases with the increasing value of *Joule* heating parameter *Jul.*

The variation of transient velocity and temperature with Prandtl number for fixed values *Jul = 0.73, λ = 0.30, Q = 0.50, N=0.75* and *γ = 0.10* are shown in Figure 14 and Figure 15. It is observed that the time taken to reach the temporal maximum and steady state increases with the increasing value of Prandtl number parameter *Pr* of the fluid. From the numerical results, we observe that the velocity profile increases with the increasing value of Prandtl's number parameter *Pr*.

The assessment of derivatives using a five-point approximation formula is included in "EQ" (12), (14), (15), and (16), followed by the evaluation of integrals using the

Newton-Cotes closed integration formula. The local skin-friction values are calculated using "EQ" (13) and plotted as a function of the axial coordinate λ as well as selected values of the variation parameters λ, γ, Q, N, and Jul in Figure 16. The local skin friction increases as the temperature rises. Local skin friction appears to diminish as the value of the viscous variation parameter λ increases. It's also worth mentioning that the local wall shear stress increases as the value of the heat conductivity parameter γ rises.

Figure 17 shows a dimensionless steady state local heat transfer rate for various values of variance parameters. As the viscosity, thermal conductivity properties rise, the rate of local heat transfer increases. As Pr rises, the rate of local heat transfer rises as well.

5. Conclusions

This study investigates the influence of temperature-dependent viscosity and thermal conductivity on heat generation in laminar natural convection boundary-layer flow along a vertical plate, incorporating the effect of Joule heating, characterized by the parameter Jul. The fluid viscosity is modeled as an exponential function of temperature, while thermal conductivity is assumed to vary linearly with temperature. The dimensionless governing equations are discretized and solved using an implicit Crank–Nicolson finite difference scheme. Numerical results are validated through graphical comparison with previously published studies, demonstrating excellent agreement and confirming the accuracy of the computational approach. The analysis reveals the following key findings:

i. **Effect of Viscosity Variation**: An increase in the viscosity variation parameter enhances the dimensionless velocity near the wall, particularly at lower fluid temperatures. This behavior leads to a higher local Nusselt number and reduced skin friction, indicating improved heat transfer performance.
ii. **Effect of Thermal Conductivity Variation**: As the thermal conductivity parameter increases, both the fluid temperature and velocity rise. Additionally, the wall velocity gradient and the dimensionless heat transfer rate (Nusselt number) are significantly enhanced, indicating stronger convective transport.
iii. **Importance of Variable Properties**: Neglecting the temperature dependency of viscosity and thermal conductivity introduces substantial errors in predicting flow and thermal fields. Accurate modeling of these variations is essential for reliable simulation of natural convection phenomena.
iv. **Influence of Joule Heating and Heat Generation**: Increasing the Joule heating parameter Jul slightly enhances both velocity and temperature profiles. A rise in the internal heat generation parameter Q significantly increases fluid velocity and temperature throughout the boundary layer.
v. **Combined Effects on Flow and Heat Transfer**: Simultaneous variation of Q, the pressure work parameter, and temperature-dependent viscosity and thermal conductivity leads to a decrease in the local skin friction coefficient, local Nusselt number, and velocity across the boundary layer, while the temperature field exhibits a noticeable increase.
vi. **Effect of Heat Generation Parameter Alone**: An isolated increase in Q produces a marked rise in both velocity and temperature profiles, intensifying the convective transport mechanism.
vii. **Cumulative Parameter Influence**: When all key parameters Q, Jul, variable viscosity, and thermal conductivity—are varied together, the trend shows a general decrease in local skin friction and Nusselt number, with a concurrent rise in fluid temperature, emphasizing the dominance of thermal effects over momentum diffusion.

Future studies may include the effects of magnetic fields (MHD), use of Nano fluids or hybrid Nano fluids, and extension to three-dimensional or transient models. Investigating variable surface conditions, porous media, and advanced numerical or optimization techniques could further enhance accuracy. Experimental validation is also recommended to support the numerical findings.

Conflicts of Interest

The authors declare no conflicts of interest.

REFERENCES

[1] S. P. K. Sarkar, M. M. Alam, "Effect of variable viscosity and thermal conductivity on MHD natural convection flow along a vertical flat plate. Journal of Advances in Mathematics and Computer Science," 2021, Vol. 36, No. 3, pp. 58-71.

[2] M. M. Alam, M. A. Alim, M. M. K. Chowdhury, "Effect of pressure stress work and viscous dissipation in natural convection flow along a vertical flat plate with heat conduction," Journal of Naval Architecture and Marine Engineering. 2006, Vol. 3, No. 2, pp. 69-76.

[3] M. A. Alim, M. M. Alam, Abdullah Al-Mamun, "Joule heating effect on the coupling of conduction with magneto-hydrodynamic free convection flow from a vertical flat plate," Nonlinear Analysis Modeling and Control. 2007, Vol. 12, No. 3, pp. 307-316.

[4] M. M. Rahman, A. A. Mamun, M. A. Azim, M. A. Alim, "Effects of temperature dependent thermal conductivity on MHD free convection flow along a vertical flat plate with heat conduction," Nonlinear Analysis Modeling and Control. 2008, Vol. 13, No. 4, pp. 513-524.

[5] M. A. Alim, M. M. Alam, Abdullah Al-Mamun, Belal Hossain, "The combined effect of viscous dissipation & Joule heating on the coupling of conduction & free convection along a vertical flat plate," *International Communications in Heat and Mass Transfer*. 2008, Vol. 35(3), pp. 338-346.

[6] M. M. Molla, M. A. Hossain L. S. Yao, "Natural convection flow along a vertical wavy surface temperature in presence of heat generation/absorption," *Int. J. Thermal Science*. 2004, Vol. 43, pp. 157-163.

[7] A. K. M. Safiqul Islam, M. A. Alim, M. M. A. Sarker, A. F. M. Khodadad Khan, "Effects of temperature dependent thermal conductivity on natural convection flow along a vertical flat plate with heat generation," *Journal of Naval Architecture and Marine Engineering* JNAME. Dec 2012. Vol. 9(2), pp. 113-122.

[8] K. H. Kabir, M. A. Alim, L. S. Andallah, "Effects of viscous dissipation on MHD natural convection flow along a vertical wavy surface," Journal of *Theoretical and Applied Physics. a Springer Open Journal*. June 2013, Vol. 7(31), pp. 1-8.

[9] M. A. Hossain, "Viscous and Joule heating effects on MHD free convection flow with variable plate temperature," *Int. J. Heat and Mass Transfer*. 1992, Vol. 35(2), pp. 3485-3487.

[10] V. M. Soundalgekar, P Ganesan, "Finite difference analysis of transient free convection on an isothermal flat plate," Reg. J. Energy Heat Mass Transf. 1981, 3, 219-224.

[11] E. M. A. Elbashbeshy, F. N. Ibrahim, "Steady free convection flow with variable viscosity and thermal diffusivity along a vertical plate," J. Phys. D Appl. Phys. 1993, 26(12), 237-2143.

[12] N. G. Kafoussius, D. A. S Rees, "Numerical study of the combined free and forced convective laminar boundary layer flow past a vertical isothermal flat plate with temperature dependent viscosity," Acta Mech. 1998, 127(11), 39-50.

[13] M. Anwar Hossain, K. Khalil, V Kambi, "The effect of radiation on free convection flow of fluid with variable viscosity from a porous vertical plate," Int. J. Therm. Sci. 2001, 40, 115-124.

[14] M. A. Seddeek, "Effect of variable viscosity on a MHD free convection flow past a semi-infinite flat plate with an aligned magnetic field in the case of unsteady flow," Int. J. Heat Mass Transf. 2002, 45, 931-935.

[15] G. Palani, Kwang, "Numerical study on vertical plate with variable viscosity and thermal conductivity," Springer-Verlag. 2009, Vol. 80, pp. 711-725.

[16] J. C. Siattery, "Momentum, energy and mass transfer in continua," McGraw Hill, New York. 1972.

[17] H. Ockendon, J. R. Ockendon, "Variable viscosity flows in heated and cooled channels," J. Fluid Mech. 1977, 83(1), 177-190.

[18] E. M. A Elbashbeshy, M. F. Dimian, "Effect of radiation on the flow and heat transfer over a wedge with variable viscosity," Appl. Math. Comput. 2002, 132, 445-454.

[19] M. A. Seddeek, M. S. Abdelmeguid, "Effects of radiation and thermal diffusivity on heat transfer over a stretching surface with variable heat flux," Phys. Lett. A. 2006; 348(3-6), 172-179.

[20] K. Balamurugan, R. Karthikeyan, "Viscous dissipation effect on steady free convection flow past a semi-infinite flat plate in the presence of magnetic field," International Journal of Review and Research in Applied Sciences and Engineering. 2013, Vol. 3, pp. 23-27.

[21] G. Borah, G. C. Hazarika, "Effects of variable viscosity & thermal conductivity on steady free convection flow along a semi-infinite vertical plate (in presence of uniform transverse magnetic field)," Journal of computer & Mathematical Science. 2010, Vol. 6, pp. 732-739.

[22] G. M. Abdel-Rahman, "Effects of variable viscosity and thermal conductivity on unsteady MHD flow of non-Newtonian fluid over a stretching porous sheet," Thermal Science. 2013, Vol. 17, pp. 1035-1047.

[23] M. M. Alam, M. A. Alim, M. M. K. Chowdhury, "Free convection from a vertical permeable circular cone with pressure work and non-uniform surface temperature," Nonlinear Analysis Modelling and Control. 2007, Vol. 12, pp. 21-32.

[24] S. Aktar, Mahmuda Binte Mostafa Ruma, M. A. Alim, "Conjugate effects of heat and mass transfer on natural convection flow along an isothermal sphere with radiation heat loss was," Open Journal of Fluid Dynamics. 2013. Vol. 3, pp. 86-94.

[25] R. Nasrin, M. A. Alim, "MHD free convection flow along a vertical flat plate with thermal conductivity and viscosity depending on temperature," Journal of Naval Architecture and Marine Engineering. 2009, Vol. 6, pp. 72-83.

[26] M. Miraj, M. A. Alim, M. A. H. Mamun, "Effect of viscous dissipation and radiation on natural convection flow on a sphere in presence of heat generation," International Communications in Heat and Mass Transfer. 2010, Vol. 37, pp. 660–665.

[27] M. R. Haque, M. M. Ali, M. M. Alam, M. A. Alim, "Effect of viscous dissipation on Natural convection flow over a sphere with temperature dependent thermal conductivity," Journal of Computer and Mathematical Science. 2014, Vol. 5, pp. 5-14.

[28] B. Gebhart, "Effects of viscous dissipation in natural convection," Journal of Fluid Mechanics Volume 14, 1962, pp. 225-232.

[29] A. Pozzi, and M. Lupo, "The coupling of conduction with laminar natural convection along a flat plate," International Journal Heat Mass Transfer. 1988, 31(9), pp. 1807-1814.

[30] Al-Mahasne Mayas Mohammad, Ibrahim Abu Alshaikh, Nabil Beithou1, Nasser Abdellatif, Mohammad BaniKhaled, Mohd Mansour, Magdalena Joka Yildiz, "Variable Temperature Plate Heat Transfer: MHD Fluid Natural Convection Flow in Porous Medium," Journal of Advanced Research in Numerical Heat Transfer. 2025, Volume 35, Issue 1 (2025) 88-100. https://doi.org/10.37934/arnht.35.1.88100.

[31] Iqbal Athal, Ioannis E. Sarris, Palani Velusamy, Vediyappan Govindan, "Viscosity dissipation and mixed convection flow in a vertical double-passage channel with permeable fluid. Frontiers in Nanotechnology," 2023, Front. Nanotechnol. 4: 1058973, https://doi.org/10.3389/fnano.2022.1058973.

[32] Md. Farhad Hasan, Md. Mamun Molla, Md. Kamrujjaman, Sadia Siddiqa, "Natural Convection Flow over a Vertical Permeable Circular Cone with Uniform Surface Heat Flux in Temperature-Dependent Viscosity with Three-Fold Solutions within the Boundary Layer," MDPI Computation. 2022, Computation 2022, 10, 60, https://doi.org/10.3390/computation 10040060.

[33] Sujit Mishra, Aditya Kumar Pati, Ashok Misra, Saroj Kumar Mishra, "Thermal performance of nanofluid flow along an isothermal vertical plate with velocity, thermal, and concentration slip boundary conditions employing buongiorno's revised non-homogeneous model," East European Journal of Physics. 2024, Phys. 4. 98-106, https://doi.org/10.26565/2312-4334-2024-4-09.

[34] Uzma Ahmad, Muhammad Ashraf, A. Al-Zubaidi, Aamir Ali, Salman Saleem, “Effects of temperature dependent viscosity and thermal conductivity on natural convection flow along a curved surface in the presence of exothermic catalytic chemical reaction,” 2021, PLoS ONE16(7): e0252485, https://doi.org/ 10.1371/journal.pone.0252485.